Multi-spectral T1 Weighted Imaging and T1 Quantification using 3D Radial k-space Trajectory

Steven Kecskemeti[1], Nagesh Adluru[1], Sam Hurley[1], and Andrew Alexander[1]
[1]*University of Wisconsin, Madison, Wisconsin, United States*

Introduction Conventional T1-weighted brain imaging uses 3D inversion-recovery (IR) prepared, rapid gradient recalled sequences (fGRE), such as MP-RAGE [1]. These pulse sequences are commonly used to generate high resolution, whole-brain images with good tissue contrast determined by a single inversion time fixed *a priori*. In this study, 3D radial *k*-space sampling (VIPR [2]) replaced the standard 3D Cartesian sampling to create a novel sequence (VIPR-IR) for neuroimaging. The frequent oversampling of the center of *k*-space enables the reconstruction of more than 100 image measurements along the magnetization recovery curve following the inversion preparation pulse. Thus many images with different contrasts may be simultaneously obtained in a time similar to that of standard 3D Cartesian IR-fGRE image. The effective inversion times may be reconstructed as finely as a single fGRE TR (4-6 ms), enabling the user to retrospectively select the images with the case specific optimal contrast, thereby eliminating the need to select a single, specific inversion time prior to data acquisition. Quantitative T1 mapping was performed by fitting the image signals from the different inversion times to a theoretical signal model. VIPR-IR was demonstrated and evaluated using *in vivo* brain studies and T1 relaxation phantom measurements.

Methods A spoiled, gradient recalled IR sequence was combined with 3D radial k-space sampling. The method was implemented on a Discovery MR 750 3T (GE Healthcare). After a β=180 degree adiabatic pulse and delay T_I, N radial projections with flip angle θ were acquired. A second delay T_D occurred before application of the next inversion pulse. Angular interleaving was performed to distribute the N projections evenly across the unit sphere. Additional interleaving was performed so that the additional N views after each successive inversion pulse filled in the missing locations of k-space in an approximately uniform fashion. Sliding window reconstructions of width W were performed for each of the first (N-W) views.

The signal model assumes signal averaging in the central regions of k-space [3]. The signal in the reconstructed frame that includes projections from n=q to n=q+W-1 is given by

$$M_z(n)/(M_{eq}\,sin\theta) = M_\infty(1-A^n) + M_0A^n \qquad EQ.1$$

where $A = a^p(1-a^w)/(1-a)$, $a = \exp(-T_R/T_1)cos\theta$, $M_0 = [(1-a^N)s + (1-E_D)E_Icos\beta + (1-E_I)]/(1-sa^N)$, $s = E_DE_Icos\beta$, $E_{I,D} = \exp(-TR/T_{I,D})$, and $M_{eq,\infty}$ is the equilibrium and steady stead signals. T1 values were estimated by fitting Eq. 1 for T_1, M_{eq}, α and β. The α and β maps were then fitted to a fourth order polynomial and used to fit for T_1 and M_{eq} in Eq. 1. A 17 cm spherical phantom and four small tubes containing water doped with Gd was imaged with the VIPR-IR sequence with: FOV=240mm x 240mm, slab thickness = 200mm, acquired resolution = 1.25mm x 1.25mm x 1.25 mm, T_R/T_E = 5.6ms/2.0ms , T_I = 28ms, T_D=150, N = 147, alpha = 4°, sliding window width W=28, scan time 7.5 minutes. A fast spin echo (FSE) IR sequence with the following parameters: FOV=340mm x 340mm, pFOV = 75%, slice thickness = 5mm, TR/TE = 15s/7.32ms, ETL=16, TIs=[4000 3000 1500 1000 800 500 300 200 100 50]ms and model S=A(1-B*exp(-T1*R1)), where R1 = 1/T1, was used to estimate T1. A 10 pixel x 10 pixel ROI was used to obtain the mean and standard deviation of the T1 values.

An 8 year old boy with known cerebral palsy was imaged with the VIPR-IR sequence with the following parameters: FOV=240mm x 240mm, slab thickness =200mm, acquired resolution = 1.25mm x 1.25mm x 1.25 mm, T_R/T_E = 5.0ms/1.8ms , T_I = 58ms, T_D=350, N = 161, alpha = 8°, sliding window width W= 41, scan time 7.5 minutes. Simultaneous, multiple-contrast images and quantitative R1 maps were generated.

Results Figure 1: Select TIs (a-e) and R1 (1/T1) map (units: 1/s) (f) for the VIPR-IR method. Inversion times are: (a) 151ms, (b) 265ms, (c) 349ms, (d) 448ms, (e) 735ms. Note WM, GM and CSF are nearly nulled in frames (b), (c) and (d,) respectively. Quantitative T1 values obtained with VIPR-IR for the phantom were within 10% of those obtained with FSE-IR for T1s in the range of approximately 300ms – 1100ms. Inspection of the region with long T1 over 3200 ms revealed streak artifacts that originated from the nearby bright containers with the much shorter T1s. We suspect that the implementation of parallel imaging and constrained reconstruction may improve quantitative accuracy by reducing streak artifacts.

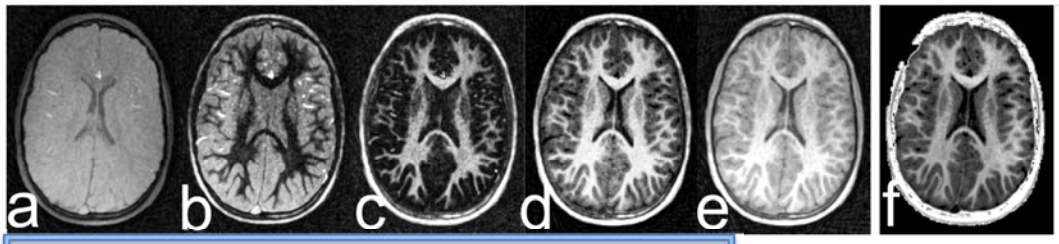

T1 Measurements in Phantom	
VIPR-IR (ms)	FSE-IR (ms)
336±3	309±3
551±13	556±4
587±7	560±4
1099±41	1034±8
2510±333	3253±314

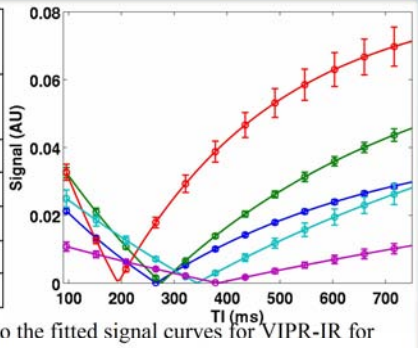

The **colored** lines correspond to the fitted signal curves for VIPR-IR for the phantoms (T1s given in table). Error bars, depicting mean and standard deviation of the signals within the ROI are plotted for every 10 points along the curve for VIPR-IR.

Discussion & Conclusions In this preliminary work we demonstrated a novel technique to obtain multiple 3D images with a wide range of IR-weighted contrasts in a single 7.5 minute scan utilizing 3D radial *k*-space sampling and sliding window reconstructions along an inversion recovery curve. Obtaining such a wide range of contrasts in a single scan may facilitate optimized, patient-specific contrast. This may improve diagnostic power when imaging pathologies with heterogeneous T1 values such as tumors or lesions. Infants and children with white matter disorders may benefit from this new technology as the T1 is unpredictable and rapidly changing in these cases. Using the same data, quantitative T1 maps may also be obtained, which will facilitate comparisons between groups and individuals and enable the estimation of contrast agent concentrations [3].

References [1] Mugler et. al, JMRI1(5):561-7 (1991) [2] Barger et al, MRM 48:297-305 (2002) [3] Kholmovski et al MRM 57:821-7 (2007)